Geomechanics and Engineering, *Vol. 37, No. 1 (2024) 9-19*
https://doi.org/10.12989/gae.2024.37.1.009

Analysis of cavity expansion based on general strength criterion and energy theory

Chao Li[1,2], Meng-meng Lu[1,2], Bin Zhu[1,2], Chao Liu[1,2], Guo-Yao Li[1,2] and Pin-Qiang Mo*[1,2]

[1]*State Key Laboratory of Intelligent Construction and Healthy Operation and Maintenance of Deep Underground Engineering, China University of Mining and Technology, Xuzhou 221116, People's Republic of China*
[2]*School of Mechanics and Civil Engineering, China University of Mining and Technology, Xuzhou 221116, People's Republic of China*

(*Received November 25, 2023, Revised March 2, 2024, Accepted March 4, 2024*)

Abstract. This study presents an energy analysis for large-strain cavity expansion problem based on the general strength criterion and energy theory. This study focuses on the energy dissipation problem during the cavity expansion process, dividing the soil mass around the cavity into an elastic region and a plastic region. Assuming compliance with the small deformation theory in the elastic region and the large deformation theory in the plastic region, combined with the general strength criterion of soil mass and energy theory, the energy dissipation solution for cavity expansion problem is derived. Firstly, from an energy perspective, the process of cavity expansion in soil mass is described as an energy conversion process. The energy dissipation mechanism is introduced into the traditional analysis of cavity expansion, and a general analytical solution for cavity expansion related to energy is derived. Subsequently, based on this general analytical solution of cavity expansion, the influence of different strength criterion, large-strain, expansion radius, cavity shape and characteristics of soil mass on the stress distribution, displacement field and energy evolution around the cavity is studied. Finally, the effectiveness and reliability of theoretical solution is verified by comparing the results of typical pressure-expansion curves with existing literature algorithms. The results indicate that different strength criterion have a relatively small impact on the displacement and strain field around the cavity, but a significant impact on the stress distribution and energy evolution around the cavity.

Keywords: cavity expansion; energy theory; general strength criterion; large-strain

1. Introduction

In order to solve practical problems encountered in engineering, many outstanding geotechnical workers have developed and applied the cavity expansion theory to solve complex geotechnical engineering problems since the 1972's, and have achieved many valuable research results. For example, explaining the resistance problem of static penetration testing (Carter *et al.*1986, Salgado and Prezzi 2007), the deformation problem of soil mass around piles (Vesic 1972, Randolph *et al.* 1979, Zhou *et al.* 2016, Zhou *et al.* 2018, Chen *et al.* 2018, Sivasithamparam and Castro 2018, Sivasithamparam and Castro 2020, Thiyyakkandi 2022), and the stability problem of tunnel excavation (Lukic *et al.* 2014, Zou *et al.* 2017, Li and Sheng 2022, Li *et al.* 2023, Kumar and Sahoo 2023), and so forth.

The solution for cavity expansion has been developed under many conditions: different strength criterion such as Tresca (Shuttle 2007), Drucker Prager (Vardoulakis and Papanastasiou 1988, Papanastasiou and Vardoulakis 1989, Papanastasiou and Vardoulakis 1992, Papanastiou and Durban 1997a, Durban and Papanastiou 1997b, Zervos and Papanastasiou 2001, Zervos *et al.* 2007, Patsalides and Papanastasiou 2019), Mohr Coulomb (Yu and Houlsby 1991, Frikha and Bouassida 2013), and spatially mobilized plane (SMP) (Matsuoka and Nakai 1974, Matsuoka 1981, Matsuoka and Sun 1995), and the Unified Strength Theory (Zhao *et al.* 2018, Zhao *et al.* 2020); and different characteristics of soil mass, such as small strain (Hughes *et al.* 1977), large-strain (Yu and Houlsby 1991), strain-softening (Cui *et al.* 2022), and three-dimensional strength of soil mass (Li *et al.* 2016).

However, there are still two issues that should not be ignored in the analysis of cavity expansion mentioned above. The first is that most researchers proposed the theoretical analysis of cavity expansion problem based on different strength criterion, but currently there are few literatures analyzing the differences in calculation results caused by different strength criterion. In addition, the possibility of establishing a general algorithm of cavity expansion is also the development direction of cavity expansion theory. The second point is that there is currently little research on the energy evolution of the cavity expansion process in published literature. For the problem of cavity expansion in sandy soil mass, Zou *et al*. (2012) proposed a solution for the ultimate expansion pressure based on nonlinear strength criterion and energy theory. Luo *et al.* (2022) further developed the solution of Zou *et al.* (2012), based on the energy dissipation method, to explain the problem of cavity expansion in compressible granular geomaterials. The above papers only studied the problem of cavity expansion in sandy soil mass, which has a relatively narrow scope of application and requires further research.

*Corresponding author, Dr.
E-mail: pinqiang.mo@cumt.edu.cn

ISSN: 2005-307X (Print), 2092-6219 (Online)

In summary, based on the general strength criterion of soil mass and energy theory, this study describes the cavity expansion process in soil mass as an energy conversion process from an energy perspective. The energy dissipation mechanism is introduced into traditional cavity expansion analysis, and a general analytical solution for cavity expansion related to energy theory is derived. Subsequently, the influence of different strength criterion and characteristics of soil mass on the stress field, displacement field and energy evolution around the cavity was considered in this solution. Finally, some data are conducted to verify the suitability of this study.

2. Theory and methodology

2.1 General strength criterion

Lade conducted an in-depth study on the strength criteria of soil mass in the 1970s (Lade et al. 1977), and proposed a general strength criterion for soil mass. The expression of strength criterion is

$$\frac{\sigma_1+\sigma_0}{\sigma_3+\sigma_0}=\mathrm{N} \tag{1}$$

where σ_1, σ_3 are the major and minor principal stresses, respectively, N, σ_0 is the strength parameter of soil mass, where $\sigma_0=c\cot\varphi$.

Corresponding to different strength criteria, the value of N varies. Here, the general strength criterion of soil mass (Lade-Duncan *et al*. 1977), Spatially Mobilized Plane (SMP) (Matsuoka and Nakai 1974, Matsuoka 1981, Matsuoka and Sun 1995), Mohr-Coulomb (M-C)) is adopted.

For the SMP criterion (Matsuoka and Nakai 1974, Matsuoka 1981, Matsuoka and Sun 1995)

$$\begin{aligned}\mathrm{N}_{SMP}&=\frac{1}{4}\left[\sqrt{8\tan^2\varphi+9}+\sqrt{8\tan^2\varphi+9-2\sqrt{8\tan^2\varphi+9}-3}-1\right]^2\\&=\frac{1}{4}\left[\sqrt{B_{SMP}}+\sqrt{B_{SMP}-2\sqrt{B_{SMP}}-3}-1\right]^2\end{aligned} \tag{2}$$

For the Lade-Duncan criterion (Lade *et al*. 1977)

$$\begin{cases}\mathrm{N}_{Lade}=\dfrac{1}{4}\left[\sqrt[3]{B_{Lade}}+\sqrt{\left(\sqrt[3]{B_{Lade}}-1\right)^2-4}-1\right]^2\\ B_{Lade}=\dfrac{I_1^3}{I_3}=\dfrac{\left(3-\sin\varphi\right)^3}{\left(1+\sin\varphi\right)\left(1-\sin\varphi\right)^2}\end{cases} \tag{3}$$

For the M-C criterion

$$\mathrm{N}_{MC}=\frac{1+\sin\varphi}{1-\sin\varphi} \tag{4}$$

where K_{SMP} and K_{Lade} are material constants, I_1, I_2 and I_3 are the first, second and third invariant of principal stress.

The limit locus of the general strength theory on the π-plane is shown in Fig. 1. As shown in Fig. 1, the M-C criterion has the smallest range, the Lade Duncan criterion has the largest range, and the SMP criterion has a range between the two.

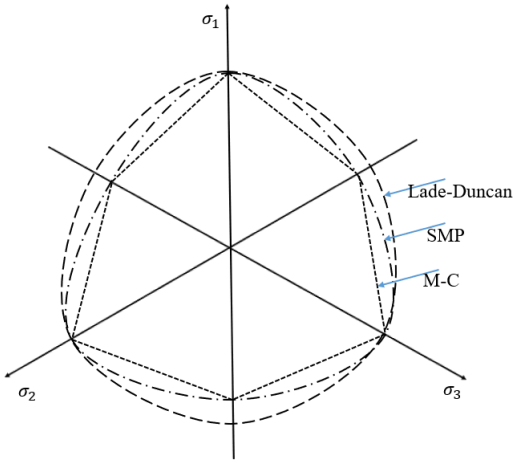

Fig. 1 Limit locus of the general strength criterion on the π-plane

For cavity expansion problem, the stress satisfies the condition that $\sigma_1 = \sigma_r$ (the radial stress), $\sigma_3 = \sigma_\theta$ (the tangential stress), the above Eq. (1) becomes (Zhao *et al*. 2018),

$$\sigma_r=N\sigma_\theta+\left(N-1\right)\sigma_0 \tag{5}$$

2.2 Problem definition

In Fig. 2, the cavity is assumed to be initially subjected to an initial horizontal pressure p_0, the external initial horizontal stress is also commonly expressed as σ_{h0}. The stress distribution of soil mass around the cavity is divided into two regions: the plastic region ($r \le r_{b0}$) and elastic region ($r>r_{b0}$), as shown in Fig. 2. Assuming that there is an initial cavity (radius a_0) in infinite soil mass under the uniform pressure p, as this pressure p gradually increases to the soil yield strength p_y, the soil mass around the cavity will transition from an elastic state to a plastic state. As the pressure p continues to increase, plastic flow will gradually occur in the soil mass within the plastic region until the internal pressure p increases to the limit expanding pressure p_u, at this point, the radius of the cavity is a_u, the range of the plastic region is $a_u<r<r_b$, and the range of the elastic region is $r \ge r_p$.

The problem of cavity expansion can be assumed as a process of energy dissipation under isothermal conditions. When the cavity pressure p is less than the critical plastic pressure p_{cr}, the work done W is small by the external force, and the soil mass around the cavity only produces elastic compression deformation, at this moment W is converted into elastic strain energy U_e. When $P>P_{\mathrm{cr}}$, the soil mass around the cavity produces elastic and plastic deformation, which is converted into elastic and plastic strain energy U_p.

The equilibrium equation for cavity expansion can be expressed as

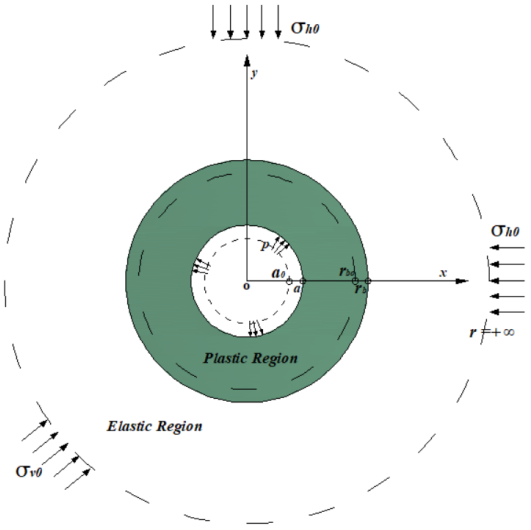

Fig. 2 The sketch for cavity expansion problem

$$\frac{d\sigma_r}{dr}+k\frac{\sigma_r-\sigma_\theta}{r}=0 \tag{6}$$

where k is constant to determine cylindrical (k=1) and spherical cavities (k=2).

2.3 Assumptions

Other assumptions can be made as follows:

(1) For elastic region, the relation of stress and strain takes the following form (Hooke's law)

$$\begin{cases} \varepsilon_r^e=\dfrac{1-\nu^2(2-k)}{E}\left(\sigma_r-\dfrac{k\nu}{1-\nu(2-k)}\sigma_\theta\right) \\ \varepsilon_\theta^e=\dfrac{1-\nu^2(2-k)}{E}\left((1-\nu(k-1))\sigma_\theta-\dfrac{\nu}{1-\nu(2-k)}\sigma_r\right) \end{cases} \tag{7}$$

where ε_r^e and ε_θ^e are the radial and tangential elastic strains in the elastic region, ν is the Poisson's ratio, E is the Young's modulus.

(2) For elastic analysis, the geometric equation can be given as

$$\left.\begin{aligned} \varepsilon_r&=-\frac{du_r}{dr} \\ \varepsilon_\theta&=-\frac{u_r}{r} \end{aligned}\right\} \tag{8}$$

(3) The large-strain can be given as

$$\left.\begin{aligned} \varepsilon_r&=-\ln\left(\frac{dr}{dr_0}\right) \\ \varepsilon_\theta&=-\ln\left(\frac{r}{r_0}\right) \end{aligned}\right\} \tag{9}$$

(4) The stresses are subject to the inner and exterior boundary conditions: $\sigma_r(r=a)=p$; $\sigma_r(r=+\infty)=p_0$; the value of stress σ_r at $r=r_b$ and $r=a_u$ equal to the value of "the soil yield strength" p_y and the value of the pressure p_u, respectively."

2.4 Elastic region

In Fig. 3, a cavity is assumed to be initially subjected to an initial inner pressure p_0, and an initial exterior stress σ_{h0}. Loading analysis, the cavity with an initial radius α_0 expand to a radius of a when the pressure is gradually increased from p_0 to p. The soil mass of cavity with the radius a is in elastic state considering the pressure, the cavity can be simplified as a plane strain problem.

The displacement and stresses in the elastic state are written

$$\begin{cases} \sigma_r=\sigma_{h0}+(p-\sigma_{h0})\left(\dfrac{a}{r}\right)^{k+1} \\ \sigma_\theta=\sigma_{h0}-\dfrac{1}{k}(p-\sigma_{h0})\left(\dfrac{a}{r}\right)^{k+1} \\ u_r=\dfrac{(\sigma_{h0}-p_0)}{2kG}r\dfrac{a^k}{r} \end{cases} \tag{10}$$

where u_r is the radial displacement around the cavity, G is the shear modulus, and E=2(1+ν)G, ν is the Poisson's ratio.

Combining the geometric equation (Eqs. (7) and (10))

$$\begin{cases} \varepsilon_{r1}^e=\dfrac{1-\nu^2(2-k)}{E}\left(\sigma_r-\dfrac{k\nu}{1-\nu(2-k)}\sigma_\theta\right) \\ \quad=\dfrac{1-\nu^2(2-k)}{E}\left(\left(1-\dfrac{k\nu}{1-\nu(2-k)}\right)\sigma_{h0}\right. \\ \quad\left.+\left(1+\dfrac{k\nu}{1-\nu(2-k)}\dfrac{1}{k}\right)(p-\sigma_{h0})\left(\dfrac{a}{r}\right)^{k+1}\right) \\ \varepsilon_{\theta1}^e=\dfrac{1-\nu^2(2-k)}{E}\left(\sigma_\theta-\dfrac{k\nu}{1-\nu(2-k)}\sigma_r\right) \\ \quad=\dfrac{1-\nu^2(2-k)}{E}\left(\left(1-\dfrac{k\nu}{1-\nu(2-k)}\right)\sigma_{h0}\right. \\ \quad\left.-\left(\dfrac{1}{k}+\dfrac{k\nu}{1-\nu(2-k)}\right)(p-\sigma_{h0})\left(\dfrac{a}{r}\right)^{k+1}\right) \\ u_{r1}=-r\varepsilon_\theta^e=-\dfrac{1-\nu^2(2-k)}{E}\left(\sigma_\theta-\dfrac{k\nu}{1-\nu(2-k)}\sigma_r\right) \\ \quad=-\dfrac{1-\nu^2(2-k)}{E}\left(\left(1-\dfrac{k\nu}{1-\nu(2-k)}\right)\sigma_{h0}r\right. \\ \quad\left.-\left(\dfrac{1}{k}+\dfrac{k\nu}{1-\nu(2-k)}\right)(p-\sigma_{h0})r\left(\dfrac{a}{r}\right)^{k+1}\right) \end{cases} \tag{11}$$

or, in the other form

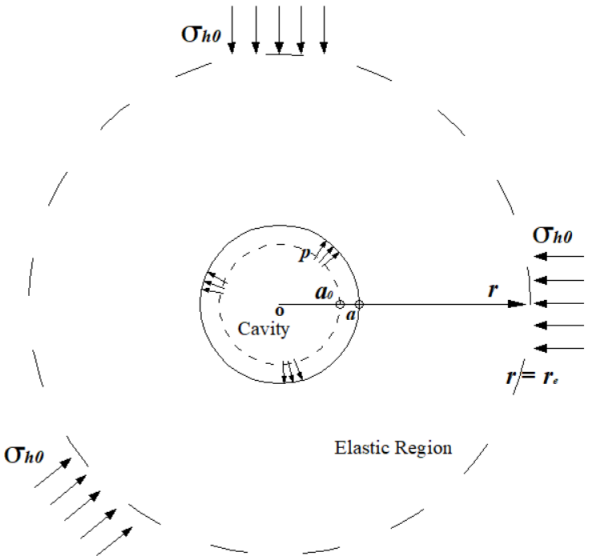

Fig. 3 Elastic loading model for cavity expansion

$$\begin{cases}\varepsilon_{r1}^{e}=\dfrac{1-\nu^2(2-k)}{E}\left(\sigma_r-\dfrac{k\nu}{1-\nu(2-k)}\sigma_\theta\right)\\ =\dfrac{1-\nu^2(2-k)}{E}\left(\begin{array}{l}\left(1-\dfrac{k\nu}{1-\nu(2-k)}\right)\sigma_{h0}\\ +\left(1+\dfrac{k\nu}{1-\nu(2-k)}\dfrac{1}{k}\right)(p_y-\sigma_{h0})\left(\dfrac{r_b}{r}\right)^{k+1}\end{array}\right)\\ \varepsilon_{\theta1}^{e}=\dfrac{1-\nu^2(2-k)}{E}\left(\sigma_\theta-\dfrac{k\nu}{1-\nu(2-k)}\sigma_r\right)\\ =\dfrac{1-\nu^2(2-k)}{E}\left(\begin{array}{l}\left(1-\dfrac{k\nu}{1-\nu(2-k)}\right)\sigma_{h0}\\ -\left(\dfrac{1}{k}+\dfrac{k\nu}{1-\nu(2-k)}\right)(p_y-\sigma_{h0})\left(\dfrac{r_b}{r}\right)^{k+1}\end{array}\right)\\ u_{r1}=-r\varepsilon_\theta^e=-\dfrac{1-\nu^2(2-k)}{E}\left(\sigma_\theta-\dfrac{k\nu}{1-\nu(2-k)}\sigma_r\right)\\ =-\dfrac{1-\nu^2(2-k)}{E}\left(\begin{array}{l}\left(1-\dfrac{k\nu}{1-\nu(2-k)}\right)\sigma_{h0}r\\ -\left(\dfrac{1}{k}+\dfrac{k\nu}{1-\nu(2-k)}\right)(p_y-\sigma_{h0})r\left(\dfrac{r_b}{r}\right)^{k+1}\end{array}\right)\end{cases}\tag{12}$$

The initial state of soil mass is isotropic

$$\begin{cases}\sigma_{r0}=\sigma_{\theta0}=\sigma_{h0}\\ \varepsilon_{r0}^{e}=\dfrac{1-\nu^2(2-k)}{E}\left(\sigma_{r0}-\dfrac{k\nu}{1-\nu(2-k)}\sigma_{\theta0}\right)\\ =\dfrac{1-\nu^2(2-k)}{E}\left(1-\dfrac{k\nu}{1-\nu(2-k)}\right)\sigma_{h0}\\ \varepsilon_{\theta0}^{e}=\dfrac{1-\nu^2(2-k)}{E}\left(\sigma_{\theta0}-\dfrac{k\nu}{1-\nu(2-k)}\sigma_{r0}\right)\\ =\dfrac{1-\nu^2(2-k)}{E}\left(1-\dfrac{k\nu}{1-\nu(2-k)}\right)\sigma_{h0}\\ u_{r0}=-r\varepsilon_{\theta0}^{e}=-\dfrac{1-\nu^2(2-k)}{E}\left(1-\dfrac{k\nu}{1-\nu(2-k)}\right)\sigma_{h0}r\end{cases}\tag{13}$$

So

$$\begin{cases}\varepsilon_r^e=\varepsilon_{r1}^e-\varepsilon_{r0}^e=\dfrac{1-\nu^2(2-k)}{E}\left(1+\dfrac{k\nu}{1-\nu(2-k)}\dfrac{1}{k}\right)(p-\sigma_{h0})\left(\dfrac{a}{r}\right)^{k+1}\\ \varepsilon_\theta^e=\varepsilon_{\theta1}^e-\varepsilon_{\theta0}^e=\dfrac{1-\nu^2(2-k)}{E}\left(\sigma_\theta-\dfrac{k\nu}{1-\nu(2-k)}\sigma_r\right)\\ =-\dfrac{1-\nu^2(2-k)}{E}\left(\dfrac{1}{k}+\dfrac{k\nu}{1-\nu(2-k)}\right)(p-\sigma_{h0})\left(\dfrac{a}{r}\right)^{k+1}\\ u_r=u_{r1}-u_{r0}=\dfrac{1-\nu^2(2-k)}{E}\left(\dfrac{1}{k}+\dfrac{k\nu}{1-\nu(2-k)}\right)(p-p_0)r\left(\dfrac{a}{r}\right)^{k+1}\\ =\dfrac{1-\nu^2(2-k)}{E}\left(\dfrac{1}{k}+\dfrac{k\nu}{1-\nu(2-k)}\right)(p-\sigma_{h0})r\left(\dfrac{a}{r}\right)^{k+1}\end{cases}\tag{14}$$

or, in the other form

$$\begin{cases}\varepsilon_r^e=\varepsilon_{r1}^e-\varepsilon_{r0}^e=\dfrac{1-\nu^2(2-k)}{E}\left(1+\dfrac{k\nu}{1-\nu(2-k)}\dfrac{1}{k}\right)(p_y-\sigma_{h0})\left(\dfrac{r_b}{r}\right)^{k+1}\\ \varepsilon_\theta^e=\varepsilon_{\theta1}^e-\varepsilon_{\theta0}^e=\dfrac{1-\nu^2(2-k)}{E}\left(\sigma_\theta-\dfrac{k\nu}{1-\nu(2-k)}\sigma_r\right)\\ =-\dfrac{1-\nu^2(2-k)}{E}\left(\dfrac{1}{k}+\dfrac{k\nu}{1-\nu(2-k)}\right)(p_y-\sigma_{h0})\left(\dfrac{r_b}{r}\right)^{k+1}\\ u_r=u_{r1}-u_{r0}=\dfrac{1-\nu^2(2-k)}{E}\left(\dfrac{1}{k}+\dfrac{k\nu}{1-\nu(2-k)}\right)(p_y-p_0)r\left(\dfrac{r_b}{r}\right)^{k+1}\\ =\dfrac{1-\nu^2(2-k)}{E}\left(\dfrac{1}{k}+\dfrac{k\nu}{1-\nu(2-k)}\right)(p_y-\sigma_{h0})r\left(\dfrac{r_b}{r}\right)^{k+1}\end{cases}\tag{15}$$

The elastic strain energy in the elastic region is given as

$$\begin{aligned}U_e&=\iiint_v v_e dV=\iiint_v\frac{1}{2}\left(\sigma_r^e\varepsilon_r^e+\sigma_\theta^e\varepsilon_\theta^e\right)dV\\ &=2\pi\int_{rb}^{\infty}\frac{1}{2}\left(\sigma_r^e\varepsilon_r^e+\sigma_\theta^e\varepsilon_\theta^e\right)rdr\\ &=2\pi\int_{rb}^{\infty}\frac{1}{2}\left(\begin{array}{l}\left(p_0+(p_y-p_0)\left(\dfrac{r_b}{r}\right)^{k+1}\right)\\ \left(\dfrac{1-\nu^2(2-k)}{E}\left(1+\dfrac{k\nu}{1-\nu(2-k)}\dfrac{1}{k}\right)(p_y-\sigma_{h0})\left(\dfrac{r_b}{r}\right)^{k+1}\right)\\ +\left(p_0-(p_y-p_0)\left(\dfrac{r_b}{r}\right)^{k+1}\right)\\ \left(-\dfrac{1-\nu^2(2-k)}{E}\left(\dfrac{1}{k}+\dfrac{k\nu}{1-\nu(2-k)}\right)(p_y-\sigma_{h0})\left(\dfrac{r_b}{r}\right)^{k+1}\right)\end{array}\right)rdr\end{aligned}\tag{16}$$

Upon loading, the first yield appeared in the cavity wall. Substituting Eq. (10) into Eq. (5), which can be obtained as follows

$$p_{cr}=p_y=\frac{\left(N+\dfrac{N}{k}\right)\sigma_{h0}+(N-1)\sigma_0}{1+\dfrac{N}{k}}\tag{17}$$

2.5 Elasto-plastic region

The Eq. (10) can also be expressed by p_y and r_b as,

$$\begin{cases}\sigma_r=\sigma_{h0}+(p_y-\sigma_{h0})\left(\dfrac{r_b}{r}\right)^{k+1}\\ \sigma_\theta=\sigma_{h0}-\dfrac{1}{k}(p_y-\sigma_{h0})\left(\dfrac{r_b}{r}\right)^{k+1}\\ u_r=\dfrac{(p_y-\sigma_{h0})}{2kG}r\left(\dfrac{r_b}{r}\right)^{k+1}\end{cases}\tag{18}$$

The radial displacement u_{rb} of the particle at the EP

(Elasto-plastic) boundary r_b can be obtained

$$\begin{cases} u_r = \dfrac{\left(p_y-\sigma_{h0}\right)}{2kG} r\left(\dfrac{r_b}{r}\right)^{k+1} = \dfrac{(N-1)\sigma_{h0}+(N-1)\sigma_0}{\left(1+\dfrac{N}{k}\right)2kG} r\left(\dfrac{r_b}{r}\right)^{k+1} \\ u_r\big|_{r=rb} = \dfrac{(N-1)\sigma_{h0}+(N-1)\sigma_0}{\left(1+\dfrac{N}{k}\right)2kG} r_b = r_b - r_{b0} \\ \Rightarrow r_{b0} = \left[1-\dfrac{(N-1)\sigma_{h0}+(N-1)\sigma_0}{\left(1+\dfrac{N}{k}\right)2kG}\right] r_b \end{cases} \tag{19}$$

2.6 Stress analysis

Combining Eqs. (5) and (6), the following equations can be derived as,

$$\frac{d\sigma_r}{dr} + k\left(\frac{N-1}{N}\right)\frac{\sigma_r+\sigma_0}{r} = 0 \tag{20}$$

Integrating Eq. (20) along r ($a \le r \le r_b$) gives (Zhao *et al.* 2018)

$$\sigma_r = \frac{1}{k\dfrac{N-1}{N}}\left(\frac{H}{r}\right)^{k\frac{N-1}{N}} - \sigma_0 \tag{21}$$

where H=constant of integration. Combining the boundary conditions,

$$\begin{aligned} H &= \left[k\frac{N-1}{N}\left(p_y+\sigma_0\right)\right]^{\frac{1}{k\frac{N-1}{N}}} r_b \\ &= \left[k\frac{N-1}{N}\left(p+\sigma_0\right)\right]^{\frac{1}{k\frac{N-1}{N}}} a \end{aligned} \tag{22}$$

The following equation can be deduced from Eq. (22)

$$\frac{r_b}{a} = \frac{\left[k\dfrac{N-1}{N}\left(p+\sigma_0\right)\right]^{\frac{1}{k\frac{N-1}{N}}}}{\left[k\dfrac{N-1}{N}\left(p_y+\sigma_0\right)\right]^{\frac{1}{k\frac{N-1}{N}}}} \tag{23}$$

Combining Eqs. (17), (18) and (23) gives

$$\begin{cases} \sigma_r = \left(p_y+\sigma_0\right)\left(\dfrac{r_b}{r}\right)^{k\frac{N-1}{N}} - \sigma_0 \\ \quad = \left(\dfrac{\left(N+\dfrac{N}{k}\right)\sigma_{h0}+(N-1)\sigma_0}{1+\dfrac{N}{k}} + \sigma_0\right)\left(\dfrac{r_b}{r}\right)^{k\frac{N-1}{N}} - \sigma_0 \\ \sigma_\theta = \dfrac{1}{N}\left(\left(p_y+\sigma_0\right)\left(\dfrac{r_b}{r}\right)^{k\frac{N-1}{N}} - \sigma_0\right) - \dfrac{N-1}{N}\sigma_0 \\ \quad = \dfrac{1}{N}\left(\left(\dfrac{\left(N+\dfrac{N}{k}\right)\sigma_{h0}+(N-1)\sigma_0}{1+\dfrac{N}{k}} + \sigma_0\right)\left(\dfrac{r_b}{r}\right)^{k\frac{N-1}{N}} - \sigma_0\right) - \dfrac{N-1}{N}\sigma_0 \end{cases} \tag{24}$$

Correspondingly, it can also be represented by p and a as

$$\begin{cases} \sigma_r = \left(p+\sigma_0\right)\left(\dfrac{a}{r}\right)^{k\frac{N-1}{N}} - \sigma_0 \\ \sigma_\theta = \dfrac{1}{N}\left(\left(p+\sigma_0\right)\left(\dfrac{a}{r}\right)^{k\frac{N-1}{N}} - \sigma_0\right) - \dfrac{N-1}{N}\sigma_0 \end{cases} \tag{25}$$

The non-associated flow rule is adopted

$$\frac{d\varepsilon_r^p}{d\varepsilon_\theta^p} = -\frac{k}{\beta} \tag{26}$$

where $\beta = \left(1+\sin\psi\right)/\left(1-\sin\psi\right)$, ψ =the dilatancy angle of soil mass, $d\varepsilon_\theta^p$ and $d\varepsilon_r^p$ are the tangential and radial plastic strain increments, respectively.

With the initial plastic strain equal to 0 and elastic strain in the plastic region ignored (Hughes *et al.* 1977), integrating Eq. (30) along the loading time series yields

$$\begin{aligned} U_p &= \iiint_V \frac{1}{2}\left(\sigma_r^p\varepsilon_r^p + \sigma_\theta^p\varepsilon_\theta^p\right)dV = 2\pi\int_a^{rb}\frac{1}{2}\left(\sigma_r^p\varepsilon_r^p + \sigma_\theta^p\varepsilon_\theta^p\right)rdr \\ &= 2\pi\int_a^{rb}\frac{1}{2}\left\{\begin{array}{l} \left(\left(p_y+\sigma_0\right)\left(\dfrac{r_b}{r}\right)^{k\frac{N-1}{N}} - \sigma_0\right)\cdot \\ \left\{-\dfrac{k}{\beta}\left\{-\ln\left\{r\Big/\left(r^{\frac{k}{\beta}+1} - r_b^{\frac{k}{\beta}+1} + \left[\left(1-\dfrac{(N-1)\sigma_{h0}+(N-1)\sigma_0}{\left(1+\dfrac{N}{k}\right)2kG}\right)r_b\right]^{\frac{k}{\beta}+1}\right)^{\frac{1}{\left(\frac{k}{\beta}+1\right)}}\right\}\right\} \\ +\left(\dfrac{1}{N}\left(\left(p_y+\sigma_0\right)\left(\dfrac{r_b}{r}\right)^{k\frac{N-1}{N}} - \sigma_0\right) - \dfrac{N-1}{N}\sigma_0\right)\cdot \\ \left\{-\ln\left\{r\Big/\left(r^{\frac{k}{\beta}+1} - r_b^{\frac{k}{\beta}+1} + \left[\left(1-\dfrac{(N-1)\sigma_{h0}+(N-1)\sigma_0}{\left(1+\dfrac{N}{k}\right)2kG}\right)r_b\right]^{\frac{k}{\beta}+1}\right)^{\frac{1}{\left(\frac{k}{\beta}+1\right)}}\right\}\right\} \end{array}\right\} rdr \end{aligned} \tag{32}$$

(Zhao *et al*. 2020)

$$\frac{\varepsilon_r}{\varepsilon_\theta} \cong \frac{\varepsilon_r^p}{\varepsilon_\theta^p} = -\frac{k}{\beta} \tag{27}$$

Substituting the large-strain equation into Eq. (27) and integrating in the plastic region, the relation that the particle at r=r_0 before and after cavity should satisfy can be obtained as

$$r^{\frac{k}{\beta}+1} - r_0^{\frac{k}{\beta}+1} = a^{\frac{k}{\beta}+1} - a_0^{\frac{k}{\beta}+1} = r_b^{\frac{k}{\beta}+1} - r_{b0}^{\frac{k}{\beta}+1} \tag{28}$$

Combining Eqs. (19) and (28), the displacement u_r is as

$$\begin{aligned} u_r &= r - r_0 = r - \left(r^{\frac{k}{\beta}+1} - r_b^{\frac{k}{\beta}+1} + r_{b0}^{\frac{k}{\beta}+1}\right)^{1\Big/\left(\frac{k}{\beta}+1\right)} \\ &= r - \left(r^{\frac{k}{\beta}+1} - r_b^{\frac{k}{\beta}+1} + \left[\left(1-\frac{(N-1)\sigma_{h0}+(N-1)\sigma_0}{\left(1+\dfrac{N}{k}\right)2kG}\right)r_b\right]^{\frac{k}{\beta}+1}\right)^{1\Big/\left(\frac{k}{\beta}+1\right)} \end{aligned} \tag{29}$$

hence, Eq. (29) is the elasto-plastic displacement field of cavity expansion accounting for the large-strain in the plastic region.

2.7 The radial and tangential strains in the plastic region

Based on the Eq. (29), the following equations can be obtained

$$\begin{cases} \dfrac{r}{r_0}=\dfrac{r}{\left(r^{\frac{k}{\beta}+1}-r_b^{\frac{k}{\beta}+1}+\left[\left(1-\dfrac{(N-1)\sigma_{h0}+(N-1)\sigma_0}{\left(1+\dfrac{N}{k}\right)2kG}\right)r_b\right]^{\frac{k}{\beta}+1}\right)^{1/\left(\frac{k}{\beta}+1\right)}} \\ \varepsilon_\theta=-\ln\left(\dfrac{r}{r_0}\right)=-\ln\left\{r\Big/\left(r^{\frac{k}{\beta}+1}-r_b^{\frac{k}{\beta}+1}+\left[\left(1-\dfrac{(N-1)\sigma_{h0}+(N-1)\sigma_0}{\left(1+\dfrac{N}{k}\right)2kG}\right)r_b\right]^{\frac{k}{\beta}+1}\right)^{1/\left(\frac{k}{\beta}+1\right)}\right\} \end{cases} \tag{30}$$

So, the radial and tangential strains in the plastic region can be obtained as

$$\begin{cases} \varepsilon_\theta=-\ln\left(\dfrac{r}{r_0}\right)=-\ln\left\{r\Big/\left(r^{\frac{k}{\beta}+1}-r_b^{\frac{k}{\beta}+1}+\left[\left(1-\dfrac{(N-1)\sigma_{h0}+(N-1)\sigma_0}{\left(1+\dfrac{N}{k}\right)2kG}\right)r_b\right]^{\frac{k}{\beta}+1}\right)^{1/\left(\frac{k}{\beta}+1\right)}\right\} \\ \varepsilon_r=-\dfrac{k}{\beta}\left\{-\ln\left\{r\Big/\left(r^{\frac{k}{\beta}+1}-r_b^{\frac{k}{\beta}+1}+\left[\left(1-\dfrac{(N-1)\sigma_{h0}+(N-1)\sigma_0}{\left(1+\dfrac{N}{k}\right)2kG}\right)r_b\right]^{\frac{k}{\beta}+1}\right)^{1/\left(\frac{k}{\beta}+1\right)}\right\}\right\} \end{cases} \tag{31}$$

2.8 Energy dissipation analysis in the plastic region

The dissipated energy in the plastic region is given as

$$\begin{aligned} U_p &= \iiint_V \frac{1}{2}\left(\sigma_r^p\varepsilon_r^p+\sigma_\theta^p\varepsilon_\theta^p\right)dV=2\pi\int_a^{r_b}\frac{1}{2}\left(\sigma_r^p\varepsilon_r^p+\sigma_\theta^p\varepsilon_\theta^p\right)rdr \\ &= 2\pi\int_a^{r_b}\frac{1}{2}\left\{\begin{array}{l}\left(\left(p_y+\sigma_0\right)\left(\dfrac{r_b}{r}\right)^{\frac{N-1}{N}}-\sigma_0\right) \\ \left\{-\dfrac{k}{\beta}\left\{-\ln\left\{r\Big/\left(r^{\frac{k}{\beta}+1}-r_b^{\frac{k}{\beta}+1}+\left[\left(1-\dfrac{(N-1)\sigma_{h0}+(N-1)\sigma_0}{\left(1+\dfrac{N}{k}\right)2kG}\right)r_b\right]^{\frac{k}{\beta}+1}\right)^{1/\left(\frac{k}{\beta}+1\right)}\right\}\right\}\right\} \\ +\left(\dfrac{1}{N}\left(\left(p_y+\sigma_0\right)\left(\dfrac{r_b}{r}\right)^{\frac{N-1}{N}}-\sigma_0\right)-\dfrac{N-1}{N}\sigma_0\right) \\ \left\{-\ln\left\{r\Big/\left(r^{\frac{k}{\beta}+1}-r_b^{\frac{k}{\beta}+1}+\left[\left(1-\dfrac{(N-1)\sigma_{h0}+(N-1)\sigma_0}{\left(1+\dfrac{N}{k}\right)2kG}\right)r_b\right]^{\frac{k}{\beta}+1}\right)^{1/\left(\frac{k}{\beta}+1\right)}\right\}\right\}\end{array}\right\}rdr \end{aligned} \tag{32}$$

3. Validation and parametric study

3.1 Validation

To verify the suitability of this presented study, the value of the parameters of soil mass are adopted as follows, $E/(p_0+(p_0/2/(N-1)))=260$, the Poisson's ratio $\nu=0.3$, the internal friction angle φ=20^0, 30^0, 40^0, 50^0, and the dilation angle ψ=0^0. Figs. 4-7 show the relation of the non-dimensional expansion pressure ((*p*+ccotφ)/(*p*$_0$+ccotφ)) and the ratio *a*/*a*$_0$ with different

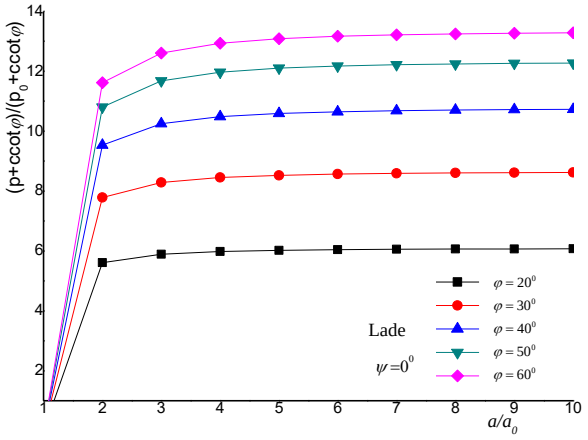

Fig. 4 Typical pressure-expansion curves using the Lade with different values φ

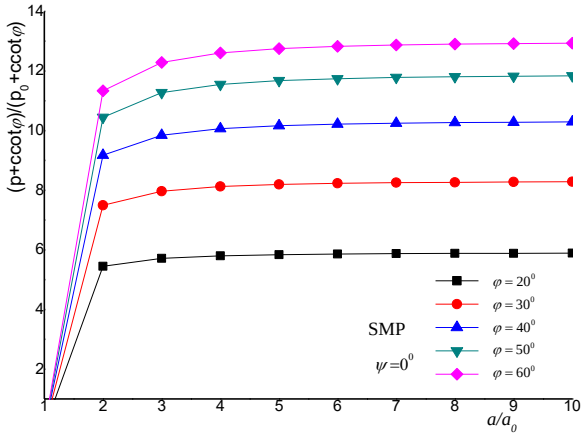

Fig. 5 Typical pressure-expansion curves using the SMP with different values φ

strength criterion and the internal friction angle. As shown in Figs. 4-6, the non-dimensional expansion pressure increases with the increase of the internal friction angle under different strength criterion. In Figs. 4-6, with the increase of *a*/*a*$_0$, the non-dimensional expansion pressure increases quickly from the start, and afterward the expansion pressure is asymptotically close to the limit pressure, as higher internal friction angles result in a wider the plastic deformation region. Fig. 7 show the relation of the non-dimensional expansion pressure ((*p*+ccotφ)/(*p*$_0$+ccotφ)) and the ratio *a*/*a*$_0$ with different strength criterion. As shown in Fig. 7, the non-dimensional expansion pressure increases with the increase of the internal friction angle under different strength criterion. The typical pressure-expansion curves from MC to SMP and then to Lade criterion show that the pressure curve obtained based on SMP and Lade criterion is greater than the pressure obtained based on MC criterion. The reason may be that SMP and Lade criterion can consider the influence of intermediate principal stress compared to MC criterion. In addition, it is shown in Fig. 7 that the curves of presented solution with ψ=30^0 and ψ=0^0 are very close to the curve of the Yu and Houlsby (1991) solution, which demonstrates the validation of the presented theoretical solution.

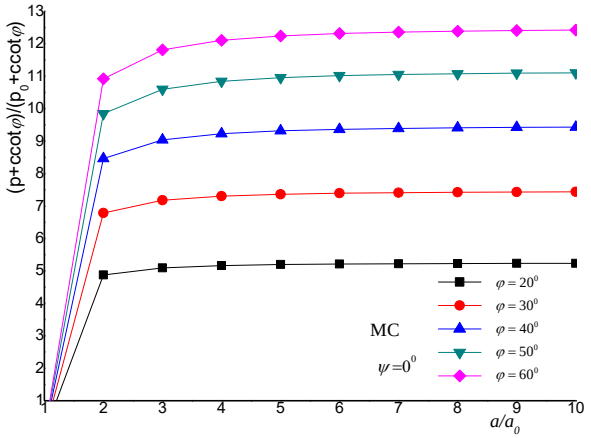

Fig. 6 Typical pressure-expansion curves using the MC with different values φ

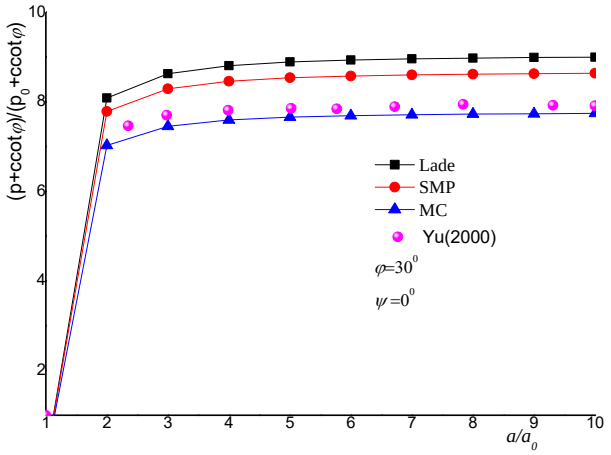

Fig. 7 Typical pressure-expansion curves using different strength criterion with φ=30^0

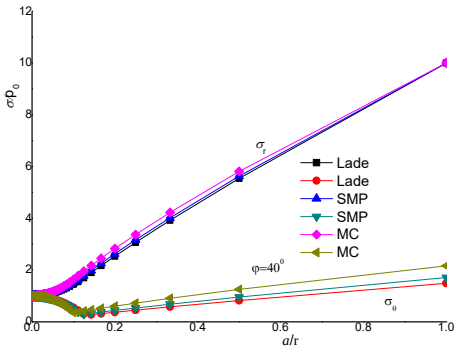

Fig. 8 Stress distribution around the cavity using different strength criterion

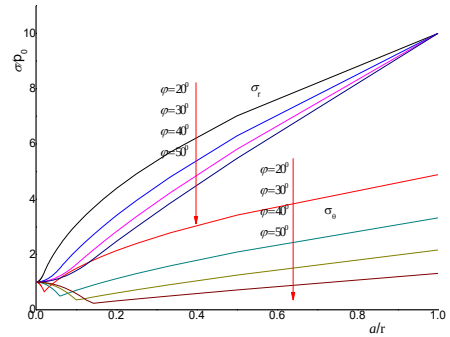

Fig. 9 Stress distribution around the cavity using the MC with different values φ

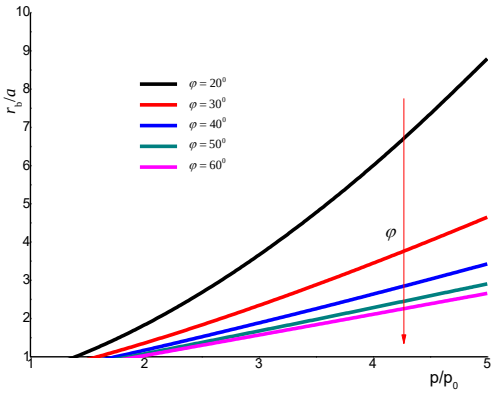

Fig. 10 Plastic radius using the Lade with different values φ

3.2 Stress distribution around cavity

3.2.1 Stress distributions

Figs. 8 and 9 shows the relation of stress distribution (σ_r, σ_θ) around the cavity and the ratio a/r with different strength criterion and the internal friction angle. From Figs. 8 and 9, it can be seen that different strength criterion and internal friction angles have an impact on both radial and tangential stresses, which the internal friction angle has a significant impact on radial and tangential stresses.

3.2.2 Plastic radius and displacement field

Figs. 10-12 show the relation of the normalized expansion pressure p/p_0 and the normalized plastic radius r_b/a with different internal friction angle. As shown in Figs. 10-12, the normalized plastic radius increases with the decrease of the internal friction angle under different strength criterion, and the increasing trend becomes more obvious as the angle decreases. Fig. 13 shows the relation of the normalized expansion pressure p/p_0 and the normalized plastic radius r_b/a with different strength criterion. As shown in Fig. 13, the normalized plastic radius curves from MC to SMP and then to Lade criterion show that the normalized plastic radius curve obtained based on SMP and Lade criterion is smaller than the normalized plastic radius obtained based on MC criterion. The reason may also be that SMP and Lade criterion can consider the influence of intermediate principal stress compared to MC criterion.

Fig. 14 shows the relation of the normalized displacement field and the radius ratio r/a with the different internal friction angle. As shown in the Fig. 14, the displacement decreases with the increase of the internal friction angle, but the decreasing trend becomes less obvious as the internal friction angle increases. Fig. 15 shows the relation of the normalized displacement field and the radius ratio r/a with different strength criterion. As shown in the Fig. 15, the normalized displacement field

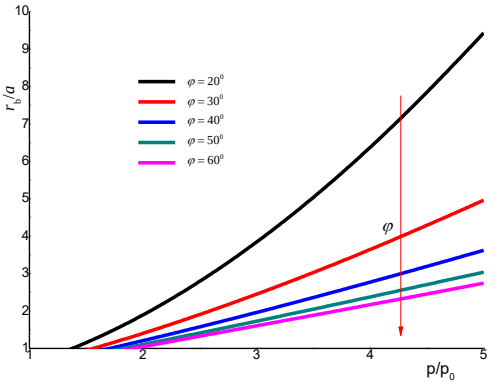

Fig. 11 Plastic radius using the SMP with different values φ

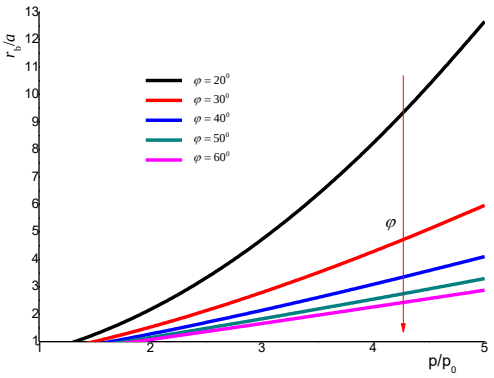

Fig. 12 Plastic radius using the MC with different values φ

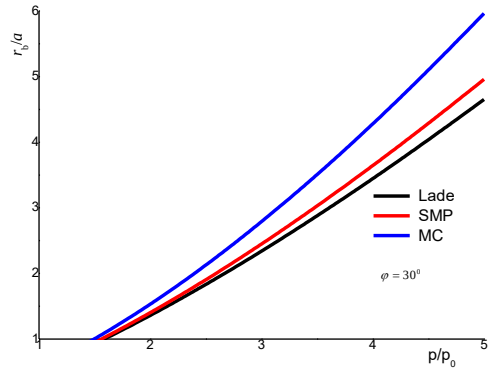

Fig. 13 Plastic radius using different strength criterion with φ=30^0

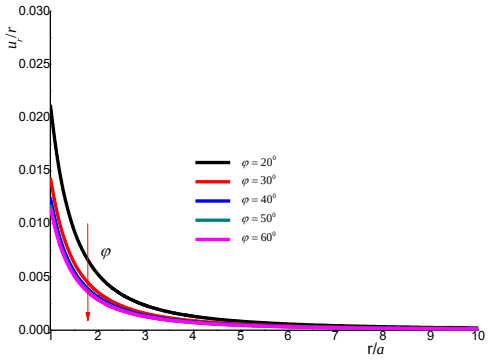

Fig. 14 Displacement field based on the SMP with different φ values

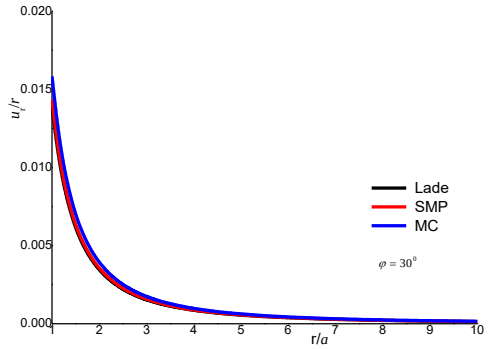

Fig. 15 Displacement field using different strength criterion with φ=30^0

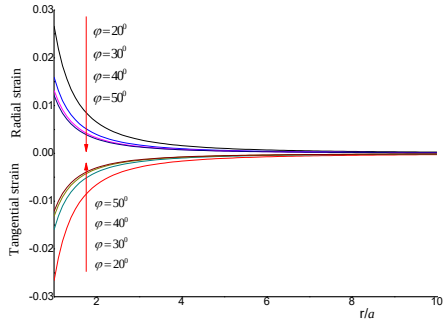

Fig. 16 Strain in the plastic region along radial direction based on the MC with different φ values

from MC to SMP and then to Lade criterion shows that although the normalized displacement obtained based on the MC criterion is the largest, it is not significant compared to the other two. In addition, it is clear that the radial displacement changes quickly in the beginning while slowly approach zero with the radial direction from Figs. 14 and 15, this is in agreement with the theoretical results reported by Zhao *et al*. (2018)

3.2.3 Strains in the plastic region

To analyze the effects of the different strength criterion and the internal friction angle on the strains in the plastic region, strains in the plastic region along radial direction with different strength criterion and internal friction angle when k=1 and k=2 are shown in Figs. 16-18. Fig. 16 shows the relation of the radial and tangential strains in the plastic region and the radius ratio r/a with the different internal friction angle. As shown in the Fig. 16, the strains decrease with the increase of the internal friction angle, but the decreasing trend becomes less obvious as the internal friction angle increases. As shown in Figs. 17, the radial and tangential strains in the plastic region almost coincide with each other under different strength criterion with φ=30^0, which illustrate that the influence of different strength criterion on the radial and tangential strains in the plastic region can be ignored. As shown in Fig. 18, under the same parameter conditions, there is a significant difference in the strain around the cavity caused by the expansion of spherical and cylindrical cavities.

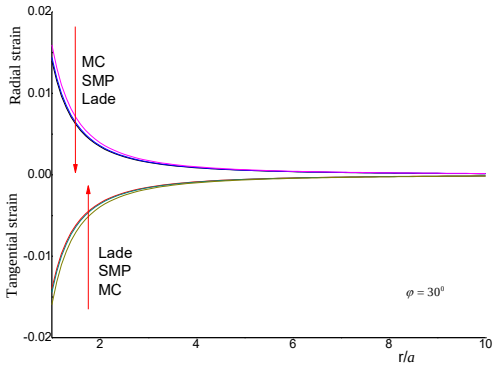

Fig. 17 Strain in the plastic region along radial direction based on different strength criterion with φ=30^0

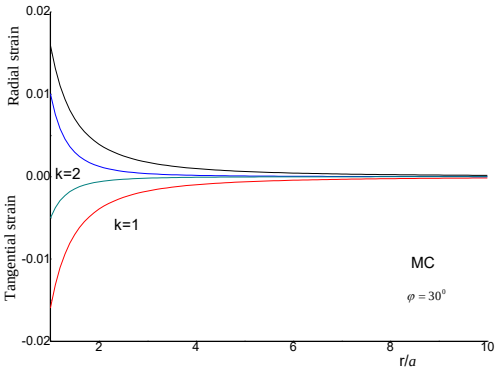

Fig. 18 Strain in the plastic region along radial direction based on the MC with k

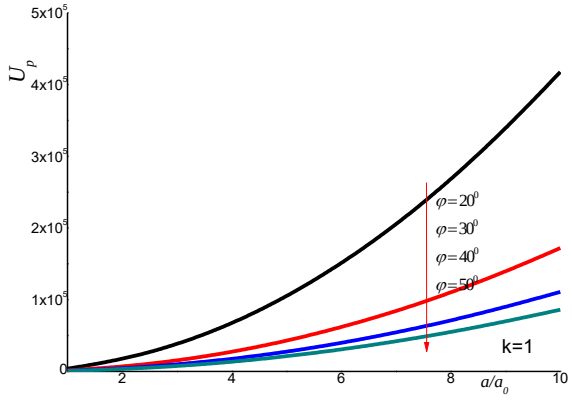

Fig. 19 The relation of dissipated energy in the plastic region and the ratio a/a_0 with different φ and k=1

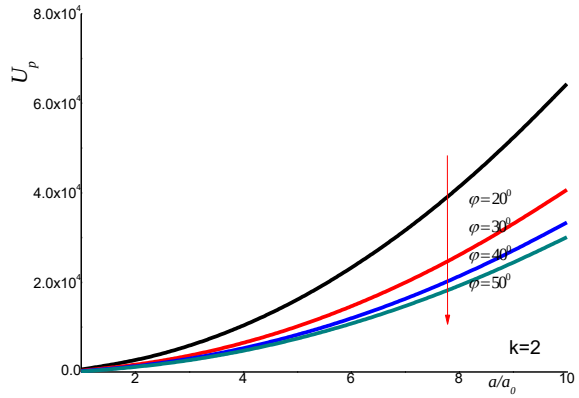

Fig. 20 The relation of dissipated energy in the plastic region and the ratio a/a_0 with different φ and k=2

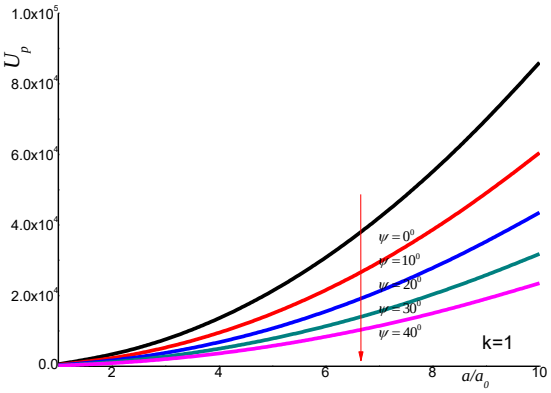

Fig. 21 The relation of dissipated energy in the plastic region and the ratio a/a_0 with different ψ

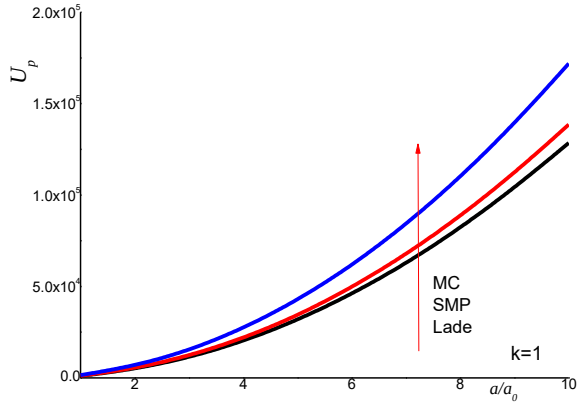

Fig. 22 The relation of dissipated energy in the plastic region and the ratio a/a_0 with different strength criterion

3.2.4 Energy dissipation analysis in the plastic region

Figs. 19-22 show the relationship of the dissipated energy in the plastic region around the cavity and the ratio a/a_0 with different strength criterion and internal friction angle when k=1 and k=2, the dissipated energy in the plastic region decreases with the increase of the internal friction angle and dilation angle, with the decrease of a/a_0, the influence of the internal friction angle and dilation angle on the dissipated energy in the plastic region become smaller and smaller until it can be ignored. From Fig. 22, it can be seen that different strength criterion have an impact on the dissipated energy in the plastic region, which the strength criterion has a significant impact on the dissipated energy in the plastic region. The dissipated energy curves from MC to SMP and then to Lade criterion show that the energy curve obtained based on SMP and Lade criterion is smaller than the energy obtained based on MC criterion.

4. Conclusions

On the basis of the general strength criterion and energy theory, an energy dissipation analysis for large-strain cavity expansion problem is described in this study. Compared

with previous solutions, the following improvements have been achieved:

(1) The presented solution for large-strain cavity expansion problem considers the effects of large-strain in the plastic region and the intermediate principal stress, which is usually ignored by most existing methods.

(2) Due to the fact that the general strength criterion of soil mass in this study includes three common failure criteria, the energy dissipation method for large-strain cavity expansion in this study has a wide range for analysis.

Acknowledgements

The authors thank Project 2022QN1019 supported by the Fundamental Research Funds for the Central Universities, and Doctor of entrepreneurship and innovation in Jiangsu Province (JSSCBS20221497), the Science and Technology Planning Project of Jiangsu Province (BK20231079), and the Foundation of State Key Laboratory of Mountain Bridge and Tunnel Engineering (Grant No. SKLBT-2213), the National Natural Science Foundation of China (Grant No. 52178374, 52209150, 52178373).

References

Carter, J.P., Booker, J.R. and Yeung, S.K. (1986), "Cavity expansion in cohesive frictional soils", *Géotechnique*, **36**(3), 349-358. https://doi.org/10.1680/geot.1986.36.3.349.

Chen, S.L. Liu, K., Castro, J. and Sivasithamparam, N. (2018), "Discussion: undrained cylindrical cavity expansion in anisotropic critical state soils", *Géotechnique*, **69**(11), 1-11, https://doi.org/10.1680/jgeot.18.D.009.

Cheng, T., Yu, Z., Zheng J., Du, J., Zhang, Y., Garg, A. and Garg, A. (2018), "Improvement of the cavity expansion theory for the measurement of strain softening in over consolidated saturated clay", *Measurement*, **119**, 156-166. https://doi.org/10.1016/j.measurement.2018.01.069.

Cui, J., Rao, P., Wu, J. and Yang, Z. (2022), "Evaluation of long term shaft resistance of the reused driven pile in clay", *Geomech. Eng.*, **29**(2), 171-182. https://doi.org/10.12989/gae.2022.29.2.171.

Durban, D. and Papanastasiou, P. (1997b), "Elastoplastic response of pressure sensitive solids, *Int. J. Numer. Anal. Meth. Geomech.*, **21**(7), 423-441. https://doi.org/10.1002/(SICI)1096-9853(199707)21:7(423::AID- NAG882)3.0.CO;2-T.

Frikha, W. and Bouassida, M. (2013), "Cylindrical cavity expansion in elastoplastic medium with a variable potential flow", *Int. J. Geomech.*, **13**(1), 19-15. https://doi.org/0.1061/(ASCE)GM.1943-5622.0000166.

Hughes, J.M.O., Wroth, C.P. and Windle, D. (1977), "Pressuremeter tests in sands", *Géotechnique*, **27**(4), 455-472. https://doi.org/10.1680/geot.1977.27.4.455.

Kumar, B. and Sahoo, J.P. (2023), "Stability assessment of unlined tunnels with semicircular arch and straight sides in anisotropic clay", *Geomech. Eng.*, **35**(2), 149-163. https://doi.org/10.12989/gae.2023.35.2.149.

Lade, P.V. (1977), "Elasto-plastic stress-strain theory for cohesionless soil with curved yield surfaces", *Int. J. Solids Struct.*, **13**(11), 1019-1035. https://doi.org/10.1016/0020-7683(77)90073-7.

Li, C. and Sheng, Y. (2022), "Large-strain analysis for cylindrical cavity contraction in strain-softening geomaterials", *Int. J. Numer. Anal. Meth. Geomech*., **46**(16), 3012-3027. https://doi.org/10.1002/nag.3439.

Li, G. Y., Mo, P.Q., Li, C., Hu, J., Zhuang, P.Z. and Yu, H.S. (2023), "Loading-unloading of spherical and cylindrical cavities in cohesive-frictional materials with arbitrary radially symmetric boundary conditions", *Appl. Math. Model.*, **124**, 488-508. https://doi.org/10.1016/j.apm.2023.07.037.

Li, J. P., Li, L. and Sun, D. A. (2016). "Analysis of undrained cylindrical cavity expansion considering three-dimensional strength of soils", *Int. J. Geomech.*, https://doi.org/10.1061/(ASCE)GM.1943-5622.0000650, 04016017.

Lukic, D.C., Prokic, A.D. and Brcic, S.V. (2014), "Stress state around cylindrical cavities in transversally isotropic rock mass", *Geomech. Eng.*, **6**(3), 213-233. https://doi.org/10.12989/gae.2014.6.3.213.

Luo, W., Li, J., Zou, J., Zhang, P. and Rong, Y. (2022), "A novel simple solution to cavity expansion problem in crushable granular materials based on energy dissipation method", *Int. J. Geomech*., **22**(2): 04021281. https://doi.org/10.1061/(ASCE)GM.1943-5622.0002271.

Matsuoka, H. and Nakai, T. (1974), "Stress-deformation and strength characteristics of soil under three different principal stresses." *Proc. Jap. Soc. Civ. Eng*., **23**(2), 59-70. https://doi.org/10.2208/jscej1969.1974.23259.

Matsuoka, H. and Sun, D.A. (1995), "Extension of spatially mobilized plane (SMP) to frictional and cohesive materials and its application to cemented sands", *Soils Found.*, **35**(4), 63-72. https://doi.org/10.3208/sandf.35.4_63.

Matsuoka, N. (1981), "Prediction of plane strain strength for soils from triaxial compression", *Proceedings of the 10th Int. Conf. Soil Mechan. Found. Engineer.*, Stockholm, Sweden: SMFE.

Papanastasiou, P. and Durban, D. (1997a), "Elastoplastic analysis of cylindrical cavity problems in geomaterials", *Int. J. Numer. Anal. Method. Geomech.*, **21**(2), 133-149. https://doi.org/10.1002/(SICI)1096-9853(199702)21:2<133: AID-NAG866>3.0.CO;2-A.

Papanastasiou, P. and Vardoulakis, I. (1989). "Bifurcation analysis of deep boreholes: II. Scale effect", *Int. J. Numer. Anal. Meth. Geomech*., **13**(2), 183-198. https://doi.org/10.1002/nag.1610130206.

Papanastasiou, P. and Vardoulakis, I. (1992), "Numerical treatment of progressive localization in relation to borehole stability", *Int. J. Numer. Anal. Meth. Geomech*., **16**(6), 389-424. https://doi.org/10.1002/nag.1610160602.

Patsalides, K. and Papanastasiou, P. (2019). "Influence of hardening and softening on limit pressure of cylindrical cavity expansion", *Int. J. Geomech*., **19**(4), 04019011. https://doi.org/10.1061/(ASCE)GM.1943-5622.0001366.

Randolph, M.F., Carter, J.P. and Wroth., C.P. (1979), "Driven piles in clay-The effects of installation and subsequent consolidation", *Géotechnique*, **29**(4), 361-393. https://doi.org/10.1680/geot.1979.29.4.361.

Salgado, R. and Prezzi, M. (2007), "Computation of cavity expansion pressure and penetration resistance in sands", *Int. J. Geomech*., **7**(4), 251-265. https://doi.org/10.1061/(ASCE)1532-3641(2007)7: 4(251).

Shuttle, D. (2007), "Cylindrical cavity expansion and contraction in Tresca soil", *Géotechnique*, **57**(3), 305-308. https://doi.org/10.1680/geot.2007.57.3.305.

Sivasithamparam, N. and Castro, J. (2018), "Undrained expansion of a cylindrical cavity in clays with fabric anisotropy: theoretical solution", *Acta Geotech.*, **13**(3), 729-746, https://doi.org/10.1007/s11440-017-0587-4.

Sivasithamparam, N. and Castro, J. (2020), "Undrained cylindrical cavity expansion in clays with fabric anisotropy and structure: Theoretical solution", *Comput. Geotech*., **120**(1), 103386. https://doi.org/10.1016/j.compgeo.2019.103386.

Thiyyakkandi, S. (2022), "Analysis of cavity expansion and contraction in unsaturated residual soils", *Geomech. Eng*., **28**(4), 405-419. https://doi.org/10.12989/gae.2022.28.4.405.

Vardoulakis, I. and Papanastasiou, P. (1988), "Bifurcation analysis of deep boreholes: I. Surface instabilities." *Int. J. Numer. Anal. Meth. Geomech*., **12**(4), 379-399. https://doi.org/10.1002/nag.1610120404.

Vesic, A.S. (1972), "Expansion of cavities in infinite soil mass", *J. Soil Mech. Found. Div.*, **98**(3), 265-290.

Yu, H.S. and Houlsby, G.T. (1991), "Finite cavity expansion in dilatant soils: Loading analysis", *Géotechnique*, **41**(2), 173-183. https://doi.org/10.1680/geot.1991.41.2.173.

Zervos A., Papanastasiou, P. and Vardoulakis, I. (2001), "Vardoulakis, Modelling of localization and scale effect in thick-walled cylinders with gradient elastoplasticity", *Int. J. Solids Struct*., **38**(30), 5081-5095. https://doi.org/10.1016/S0020-7683(00)00337-1.

Zervos, A. and Vardoulakis, I. and Papanastasiou, P. (2007), "Influence of nonassociativity on localization and failure in geomechanics based on gradient elastoplasticity", *Int. J. Geomech*., **7**(1), 63-74. https://doi.org/10.1061/(ASCE)1532-3641(2007)7:1(63).

Zhao, C., Wang, Y.B., Zhao, C., Wu, Y. and Fei, Y. (2020), "Analysis of drained cavity unloading-contraction considering different degrees of intermediate principal stress with unified strength theory", *Int. J. Geomech*., **20**(7), 04020086. https://ascelibrary.org/doi/full/10.1061/%28ASCE%29GM.1943-5622.0001703.

Zhao, C.F., Fei, Y., Zhao, C. and Jia, S.H. (2018), "Analysis of expanded radius and internal expanding pressure for undrained cylindrical cavity expansion", *Int. J. Geomech*., **18**(2), 04017139. https://ascelibrary.org/doi/full/10.1061/(ASCE)GM.1943-5622.0001058.

Zhou, H., Kong, G., Liu, H. and Laloui, L. (2018), "Similarity solution for cavity expansion in thermoplastic soil", *Int. J. Numer. Anal. Meth. Geomech.*, **42**(2), 274-294. https://doi.org/10.1002/nag.2724.

Zhou, H., Kong, G., Liu, H., Wu, Y. and Li, G. (2016), "A novel cavity expansion-based analytical tool and its potential application for energy pile foundation", *Proceedings of th 1st Int. Conf. Ene. Geotech*., https://doi.org/10.1201/B21938-57.

Zou, J.F., Chen, K.F. and Pan, Q.J. (2017), "Influences of seepage force and out-of-plane stress on cavity contracting and tunnel opening", *Geomech. Eng.*, **13**(6), 907-928. https://doi.org/10.12989/gae.2017.13.6.907.

Zou, J.F., Tong, W. and Zhao, J. (2012), "Energy dissipation of cavity expansion based on generalized non-linear failure criterion under high stresses", *J. Cent. South Univ*., **19**(5), 1419-1424. CNKI:SUN:ZNGY.0.2012-05-038. https://doi.org/10.1007/s11771-012-1158-3.

GC